Supporting Information

El-Chemaly *et al.* 10.1073/pnas.0813368106

Methods

Migration and Proliferation Assays. Human microvascular endothelial cells (HMEC)-1 (5×10^5) were placed in the upper chambers, and BALF without or with supplementation with short-fragment hyaluronan (5 mg/mL) (R&D Systems) was placed in the lower chambers of 96-well ChemoTx plates (Neuroprobe). After a 4-hour incubation at 37 °C, cells adherent to the pores were counted (1). Proliferation was assayed by reading the fluorescence generated by GFP-labeled HMEC-1 in the presence of BALF from the subjects with IPF and from healthy volunteers.

Chemokine Levels. BALF was concentrated (4×) using a centrifugal filter with a 3-kDa exclusion limit (Amicon Ultra; Millipore). Prolymphangiogenic proteins (VEGF-A, -C, and -D; MCP-1; FGF-b; HGF; TIMP-1 and -2) were measured by ELISA using SearchLight proteome arrays (Pierce Biotechnology) (2) in BALF samples from 15 subjects with IPF and 12 healthy volunteers. Protein concentration was corrected for epithelial lining fluid dilution (3).

Fluorescence-Activated Cell Sorting. Bronchoscopy and bronchoalveolar lavage were performed as described previously (4). Cells isolated from BALF were collected by centrifugation ($500 \times g$), washed, dispersed in PBS, and incubated for 30 min with antibodies CD45-FITC, CD14-APC, and CD11b-R-PE. Cell sorting was done as described previously (5).

1. Zudaire E, *et al.* (2008) The aryl hydrocarbon receptor repressor is a putative tumor-suppressor gene in multiple human cancers. *J Clin Invest* 118:640–650.
2. Moody MD, *et al.* (2001) Array-based ELISAs for high-throughput analysis of human cytokines. *Biotechniques* 31:186-190,192–194.
3. Rennard SI, *et al.* (1986) Estimation of volume of epithelial lining fluid recovered by lavage using urea as marker of dilution. *J Appl Physiol* 60:532–538.
4. Ren P, *et al.* (2007) Impairment of alveolar macrophage transcription in idiopathic pulmonary fibrosis. *Am J Respir Crit Care Med* 175:1151–1157.
5. Pacheco-Rodriguez G, *et al.* (2007) TSC2 loss in lymphangioleiomyomatosis cells correlated with expression of CD44v6, a molecular determinant of metastasis. *Cancer Res* 67:10573–10581.

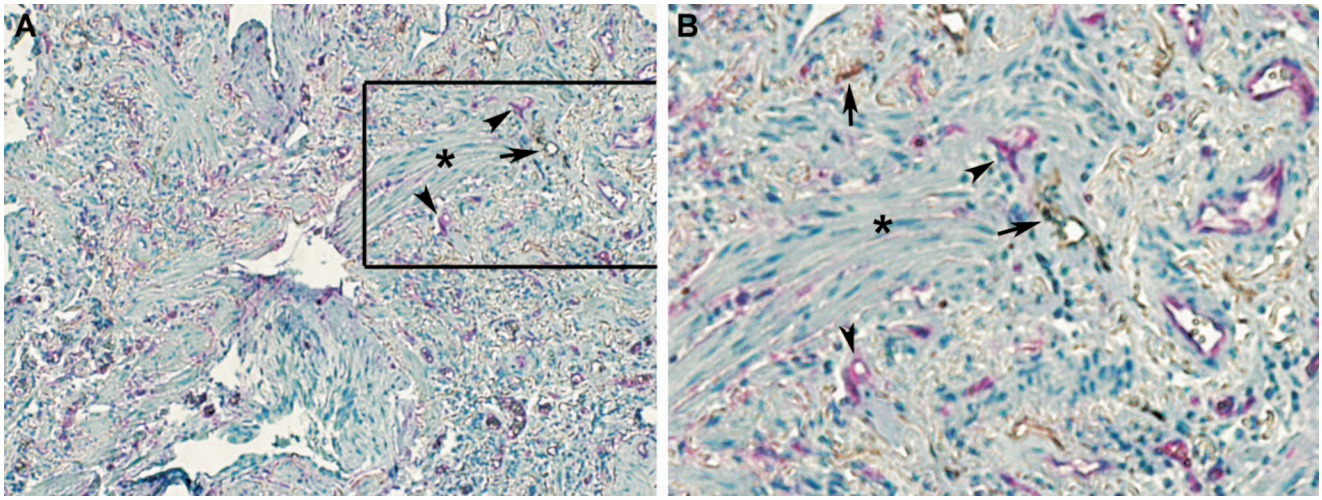

Fig. S1. Presence of lymphatic and blood vessels at the periphery of fibroblastic foci. (*A*) Reactivity with anti–D2–40 antibodies (arrow) and anti-CD34 antibodies (arrowhead) visualized with DAB and Fast Red, respectively, localized at the periphery of fibroblastic foci (*) in IPF lung tissue sections. (*B*) High magnification of a selected area highlighted in (*A*). Nuclei are stained with hematoxylin.

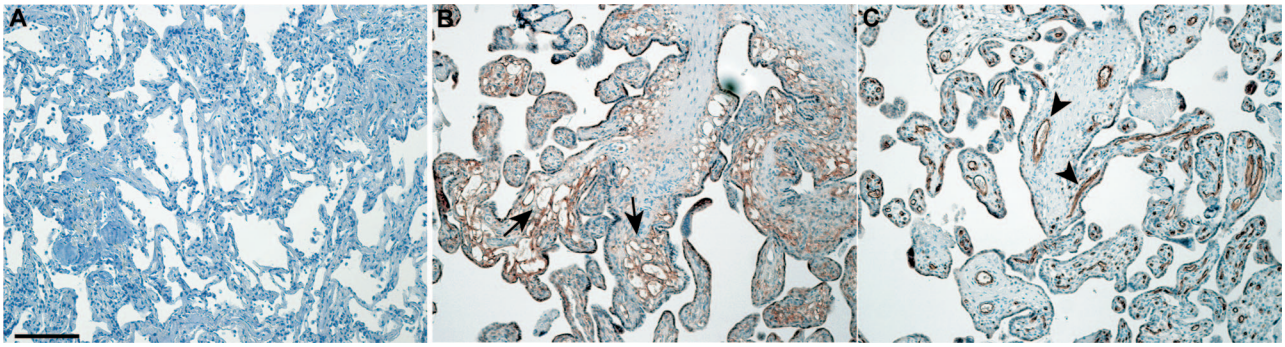

Fig. S2. Negative and positive controls for immunohistochemistry experiments. (*A*) IPF lung tissue section incubated with nonimmune IgG shows an absence of reactivity with anti–D2–40 and anti-CD34 antibodies. (*B* and *C*) Placental tissue used as a positive control demonstrates reactivity with anti–D2–40 antibodies (arrows) visualized with DAB (*B*) and reactivity with anti-CD34 antibodies (arrowheads) visualized with Fast Red (*C*). Nuclei are stained with hematoxylin.

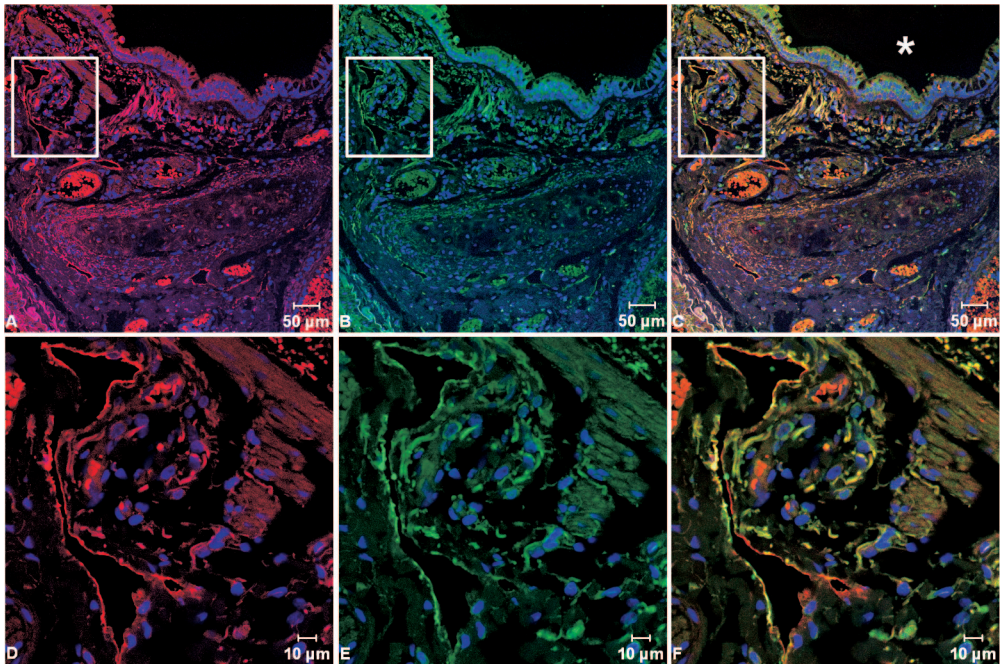

Fig. S3. In normal lung, LYVE-1 and podoplanin-positive lymphatic vessels are proximal to major vessels and airways. Immunofluorescence staining of paraffin-embedded sections of normal lung reveals podoplanin (red) and LYVE-1 (green) in lymphatic vessels. (*A–C*) Low-magnification view shows lymphatic vessels staining for both podoplanin and LYVE-1 in the proximity of large blood vessels and airways (*). (*D–F*) High- magnification images of selected boxed areas. Nuclei are stained with DAPI (blue).

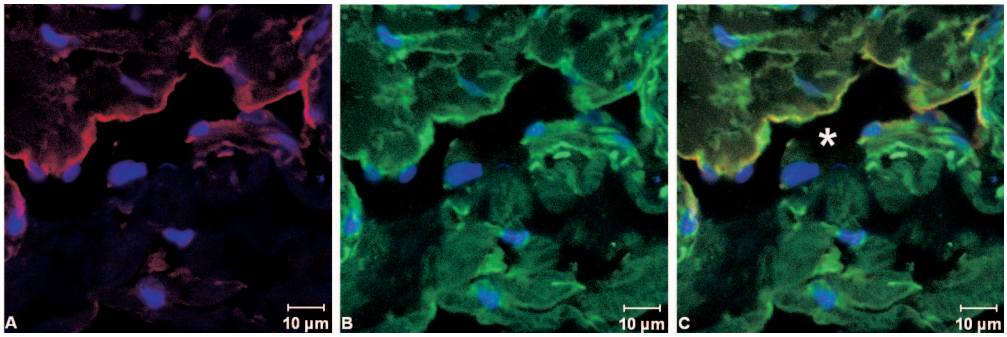

Fig. S4. Presence of LYVE-1 in podoplanin- positive lymphatic vessels in IPF lung. Immunofluorescence staining of paraffin-embedded sections of IPF lung tissue shows LYVE-1 (green) and podoplanin (red) in lymphatic vessels. (*A* and *B*) Fluorescence images show that lymphatic vessels (*) that are reactive with anti-podoplanin antibodies (*A*) are reactive with anti–LYVE-1 antibodies (*B*). (*C*) Merged DIC and fluorescence images show colocalization of podoplanin with LYVE-1. Nuclei are stained with DAPI (blue).

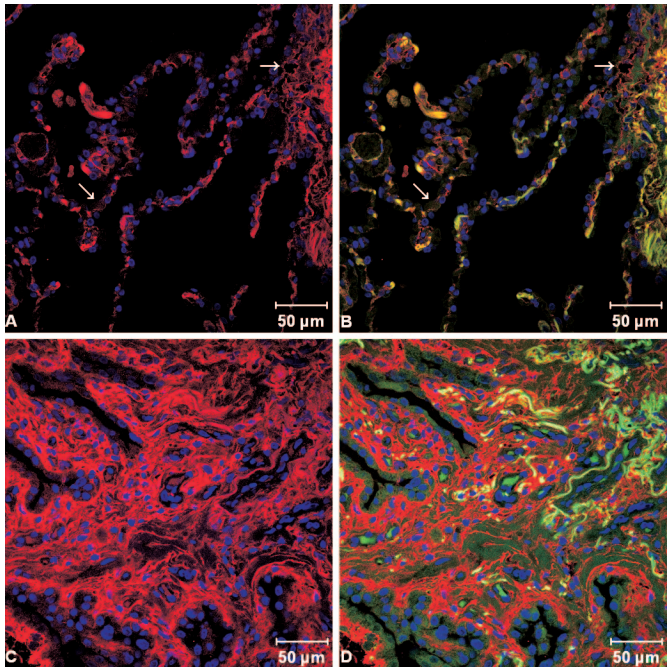

Fig. S5. IPF lung tissue sections show increased hyaluronic acid fluorescence staining compared with normal lung. Paraffin-embedded sections of normal (*A* and *B*) and IPF (*C* and *D*) lung tissue displaying staining for hyaluronic acid (red) are shown. Fluorescence images of hyaluronic acid (red) and DAPI (blue) are shown without (*A* and *C*) or with (*B* and *D*) autofluorescence signal (green). Cell nuclei are stained with DAPI (blue).

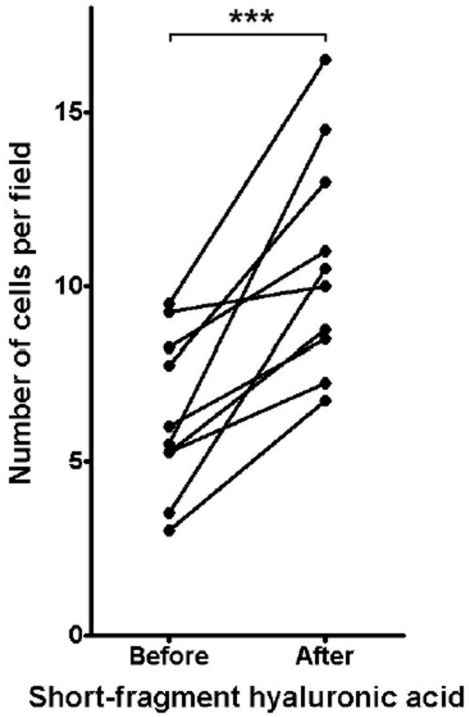

Fig. S6. BALF from healthy volunteers supplemented with short-fragment hyaluronic acid shows an increase in LEC migration. Cultured LECs were incubated with BALF from healthy volunteers without or with short-fragment hyaluronic acid (5 mg/mL). LEC migration was significantly greater in assays with BALF from healthy volunteers replenished with short-fragment hyaluronic acid (*** $P < .001$).

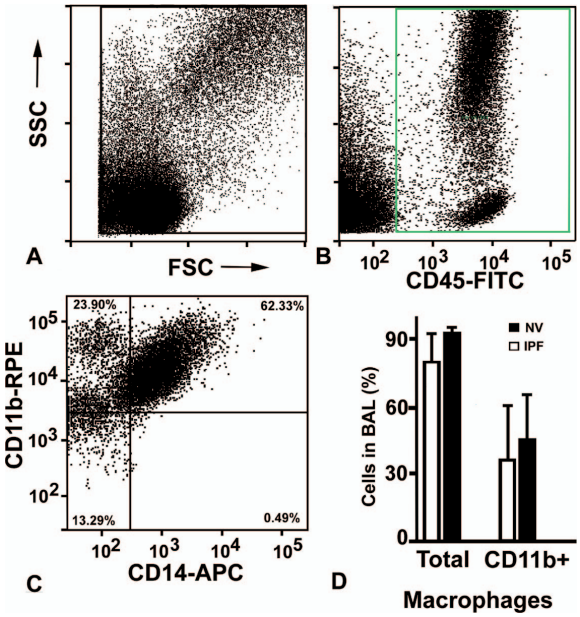

Fig. S7. Isolation of CD11b$^+$ macrophages from BALF of healthy volunteers and subjects with IPF by FACS. Cells from BALF samples were triply labeled using anti-CD45, anti-CD14, and anti-CD11b fluorescent-labeled antibodies. CD45$^+$/CD14$^+$/CD11b$^+$ cells (*C*, *Upper Right*) were collected by flow cytometry. Forward and side scatter were collected on a linear scale; fluorescent signals were collected on log scales. A broad forward- and side-scatter gate was set as shown in (*A*), followed by CD45 versus side- scatter gate, as shown in (*B*). CD14 versus CD11b was gated on both. No significant differences were found in the percentages of total alveolar macrophages and CD14$^+$/CD11b$^+$ subpopulation in BALF from subjects with IPF (white) and from healthy volunteers (black) ($P > .05$).

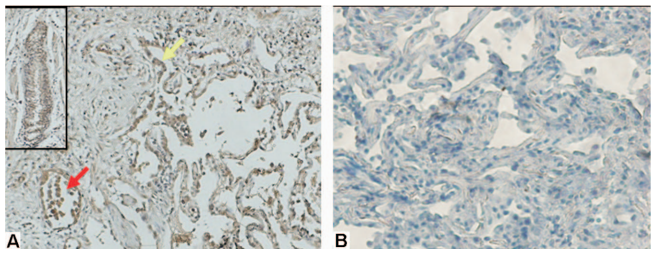

Fig. S8. Immunoreactive VEGF-C in IPF lung. (*A*) Immunoreactivity for VEGF-C visualized with diaminobenzidine (DAB) is observed in alveolar macrophages (red arrow), type II pneumocytes (yellow arrow), and airway epithelial cells (*Inset*). (*B*) Absence of immunoreactivity with nonimmune IgG.

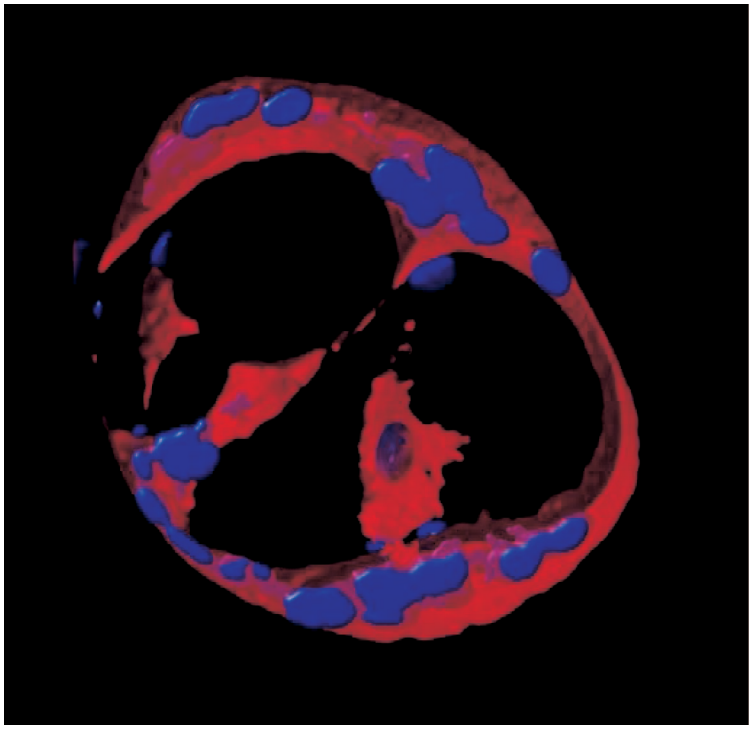

Movie S1. CD11b^{+} alveolar macrophages in IPF develop tube-like structures in vitro. Avi file compressed with DivX codec available at http://www.divx.com/.

Movie S1 (avi)

Table S1. Quantification of the number, perimeter, and area of D2–40– and CD34-positive vessels in IPF lung tissue sections

	D2–40				CD34			
	Mild (n = 3)	Moderate (n = 5)	Severe (n = 4)	*P* value*	Mild (n = 3)	Moderate (n = 5)	Severe (n = 4)	*P* value*
Number	101.6 ± 21.4	79.2 ± 16.1	83.7 ± 8.18	.18	81 ± 21.9	92 ± 31.9	169 ± 22.3	.002
Average perimeter, μm	49.2 ± 12.7	64.5 ± 8.05	81.5 ± 8.6	.005	110 ± 32.4	79.9 ± 18.5	72.8 ± 25.1	.171
Average area, μm^2	95.9 ± 46.1	117 ± 30.2	206 ± 46.5	.009	196 ± 78.2	111 ± 55.7	117 ± 53.8	.182
Total perimeter, μm	4,833 ± 465	5,092 ± 1,190	6,868 ± 1,401	.072	8,452 ± 1,147	6,994 ± 1,554	11,900 ± 2,688	.013
Total area, μm^2	9,114 ± 2,476	9,334 ± 3,522	17,379 ± 4,992	.024	14,820 ± 3,749	9,984 ± 5,439	18,823 ± 6,855	.117

**P* value based on ANOVA. A 2-way comparison showed a significant difference between the severe and mild groups.

Table S2. Characteristics of the subjects whose BALF was used for protein concentration and cell migration and proliferation experiments

	IPF subjects (n = 15)	Healthy volunteers (n = 14)
Age, years, mean ± SD	63.3 ± 11.1	41.3 ± 16.6
Males/females	13/2	8/6
Disease stage		NA
Mild	3	
Moderate	8	
Severe	4	
Medical therapy*	9	NA
Supplemental oxygen	4	NA

NA, not applicable.
*Including prednisone, immunosuppressants, IFN-γ, and/or colchicine.

Table S3. Characteristics of subjects whose BALF was collected to isolate CD11b$^+$ macrophages

	IPF subjects (n = 4)*	Healthy volunteers (n = 5)
Age, years, mean ± SD	65.8 ± 8.8	40.8 ± 11.6
Males/females	2/2	3/2
Forced expiratory volume in 1 s, % predicted, mean ± SD	98.2 ± 32.7	95.4 ± 9.0
Forced vital capacity, % predicted, mean ± SD	88.9 ± 24.3	98.0 ± 4.9
Total lung capacity, % predicted, mean ± SD	81.9 ± 17.6	101.1 ± 6.9
Diffusing capacity of the lung for CO, % predicted, mean ± SD	63.9 ± 19.7	98.5 ± 21.9

*No patients were receiving any therapy.

Table S4. Antibodies used in this study

Antigen	Application	Source
Podoplanin	Immunohistochemistry	Clone D2–40, Signet Laboratories
CD34	Immunohistochemistry	Clone QBEnd/10, Signet Laboratories
LYVE-1	Immunofluorescence	Catalog no. 11–032, AngioBio
Podoplanin	Immunofluorescence	Catalog no.11–003, AngioBio
Mouse/Rabbit IgG	Immunofluorescence	Vector Laboratories
Texas Red streptavidin	Immunofluorescence	Catalog no.016–070-084, Jackson ImmunoResearch
MCP-1	Function blocking	AF-279-NA, R&D Systems
HGF	Function blocking	AF-294-NA, R&D Systems
TIMP-1	Function blocking	9013–1008, AbD Serotec
CD45-FITC	Flow cytometry	Catalog no. 555482, BD Biosciences
CD14-APC	Flow cytometry	Catalog no. 555399, BD Biosciences
CD11b-R-PE	Flow cytometry	Catalog no. 555388, BD Biosciences